

# SYNTHESIS AND CHARACTERIZATION OF AN IN-SITU MAGNESIUM-BASED CAST NANO COMPOSITE VIA NANO-SiO<sub>2</sub> ADDITIONS TO THE MELT

## SINTEZA IN KARAKTERIZACIJA IN SITU NANOKOMPOZITA NA OSNOVI MAGNEZIJA Z NANO-SiO<sub>2</sub> DODATKOM ZA TALJENJE

Mansour Borouni<sup>1</sup>, Behzad Niroumand<sup>2</sup>, Ali Maleki<sup>3</sup>

<sup>1</sup>Isfahan University of Technology, Pardis College, Materials Engineering Group, Isfahan 84156-83111, Iran

<sup>2</sup>Isfahan University of Technology, Department of Mechanical Engineering, Isfahan, 84156-83111, Iran

<sup>3</sup>Isfahan University of Technology, Research Institute for Steel, Isfahan, 84156-83111, Iran  
m.borouni@pa.iut.ac.ir

*Prejem rokopisa – received: 2017-04-01; sprejem za objavo – accepted for publication: 2017-05-12*

doi:10.17222/mit.2017.036

In this study, AZ91C magnesium matrix in-situ nano-composites reinforced with oxide particles were produced by the addition of 2 % of mass fractions of silica nanoparticles to the melt using the stir-casting method. For this purpose, nano-silica powder was mixed in molten AZ91C by a special procedure and stirred for 15 min at 750 °C and cast in a preheated die at 720 °C. Control samples were also cast under the same conditions. Improved microstructure, reduced porosity and increased hardness, tensile strength and yield strength of the composite sample were revealed by microstructural and mechanical investigations. The hardness, yield strength and tensile strength values increased from 65 BHN, 82 MPa and 165 MPa for the monolithic samples to 77 BHN, 97 MPa and 175 MPa for the in-situ formed cast composites. Microstructural and EDS analyses suggested the in-situ formation of Al<sub>2</sub>O<sub>3</sub>, MgAl<sub>2</sub>O<sub>4</sub> and MgO oxide particles by in-situ reaction of the Al, Mg and SiO<sub>2</sub> in the melt.

Keywords: AZ91C alloy, in-situ cast nano-composite, silica nanoparticles, mechanical properties

V študiji so bili izdelani AZ91C nanokompoziti in situ, na podlagi magnezijeve matrike in ojačani z oksidnimi delci z dodatkom 2 % nanodelcev silicija za topljenje, z uporabo metode litja z mešanjem. Za ta namen je bil nanosilicijev prah zmešan v raztopljen AZ91C s posebno metodo in nato 15 min mešan na 750 °C in lit v predogretem modelu na 720 °C. Preizkušanci so bili ravnotako liti v enakih pogojih. Izboljšana mikrostruktura, zmanjšana poroznost in povečana trdota, napetostna trdnost in napetost vzorcev kompozita so bili odkriti s preiskavami mikrostrukture in z mehanskimi preiskavami. Vrednosti trdote, napetosti tečenja in natezne napetosti so se povečali iz 65 BHN, 82 Mpa in 165 MPa in za monolitne vzorce na 77 BHN, 97 MPa in 175 MPa za in situ formirane lite kompozite. Mikrostrukture in EDS-analize so predlagale in situ formacijo Al<sub>2</sub>O<sub>3</sub>, MgAl<sub>2</sub>O<sub>4</sub> in MgO oksidne delce z in situ reakcijo Al, Mg in SiO<sub>2</sub> v topljenem.

Ključne besede: AZ91C zlitina, in situ litje nanokompozitov, nanodelci silicija, mehanske lastnosti

## 1 INTRODUCTION

Besides extensive applications in automobile and aerospace industries, magnesium and its alloys have had considerable growth in three markets of communications, computer and video and photography cameras. Magnesium is the lightest industrial metal with a density of 1.74 g/cm<sup>3</sup>. Magnesium has a high specific strength and therefore it is used extensively as the metal matrix in the manufacturing of composites. Among the alloys of magnesium, Mg-Al-Zn alloys, specifically the AZ91 alloy, have extensive applications in various industries. Corrosion resistance and relatively high strength are the particular properties of the AZ91 alloy compared to other magnesium alloys. The AZ91 alloy is one of the most common magnesium alloys to produce magnesium-matrix composites.<sup>1-5</sup>

For producing magnesium-matrix composites, reinforcing materials with different shapes, sizes and materials are used. Micron-sized ceramic reinforcements including carbides, borides and oxides are the most

common.<sup>2,5</sup> Various studies are carried out in the field of magnesium-matrix composites reinforced with ceramic particles. For instance, in 2008, Hassan and Gupta produced a magnesium composite reinforced with Al<sub>2</sub>O<sub>3</sub> particles with 0.3-micron sizes using disintegrated melt deposition method and reported improved yield strength, tensile strength and flexibility by 2 % of mass fractions increase of Al<sub>2</sub>O<sub>3</sub> particles.<sup>6</sup>

By changing the scale of the reinforcing particles from micrometer to nanometer, their specific surface is increased significantly and the impact of the properties of the surface of the particles become more important. Since one of the mechanisms to increase the properties of the composites is the load transfer in the interface of the matrix and reinforcement particles, using nanoparticles, the surface of the reinforcement which is in contact with the matrix is increased and higher increases in the properties are expected.<sup>7</sup> In a research in 2012, AZ91D-TiB<sub>2</sub> nano-composites were manufactured using ultrasonic mixing and their sub-structure and mechanical properties were studied. For AZ91D nano-composites

with 2.7 % weight percentage of  $TiB_2$  with a mean diameter of 25 nanometers, the yield strength, ultimate tensile strength and plasticity were improved by 21 %, 16 %, and 48 %, respectively.<sup>8</sup>

M. Habibnejad et al.<sup>9</sup> studied producing pure magnesium and AZ31 magnesium alloy composites using  $Al_2O_3$  nano-particles by the stir-casting method. Characterization of the mechanical properties indicated that the yield strength and the tensile strength of pure magnesium and the AZ31 alloy is generally increased with nano-particles; however, the flexibility decreases.

In most of the researches, including the above-mentioned studies, the reinforcing particles are placed in the matrix in an ex-situ procedure. In in-situ composite fabrication methods, the reinforcing phase is formed during the procedure with reactions of different materials. The reaction could take place for a solid powder or in molten compounds.<sup>10</sup>

In the current study, the magnesium-matrix nano-composite AZ91C, reinforced with oxide nano-particles is produced in in-situ form by adding nano-silica particles in the molten form and the stir-casting method and the structural and mechanical properties of the produced composites are studied.

## 2 MATERIALS AND METHODS

The standard and measured (by the wet-chemistry technique) chemical compound of the alloy used in this study are shown in **Table 1**.<sup>11</sup>

**Table 1:** The chemical compound of the AZ91C alloy used in this research

% Chemical composition	Standard <sup>11</sup>	Measurement
Al	8.1-9.3	8.63
Zn	0.4-1	0.59
Mn	0.13-0.35	0.17
Si	0.3	0.1
Cu	0.1	0.05
Ni	0.01	-
Mg	Remained	Remained

In this research, silica nano-particles produced from pyrolysis and burning of HTV silicon polymer are used for the in-situ production of oxide reinforcing particles. To produce silica nano-particles, HTV silicon polymer manufactured by the Korean KCC company is used as the raw material and the production procedure is modified as done by M. Senmar et al.<sup>12</sup> In this regard, the required value of the afore-mentioned material is placed inside the resistance furnace. The furnace is warmed with a rate of 20 °C/min to reach 700 °C. Then, the material is maintained at 700 °C to be completely pyrolyzed and burnt. The resulted product is a white powder that was analyzed by X-ray diffraction (XRD), Scanning Electron Microscope (SEM) and Transmission electron microscopy (TEM). **Figure 1**, shows the x-ray

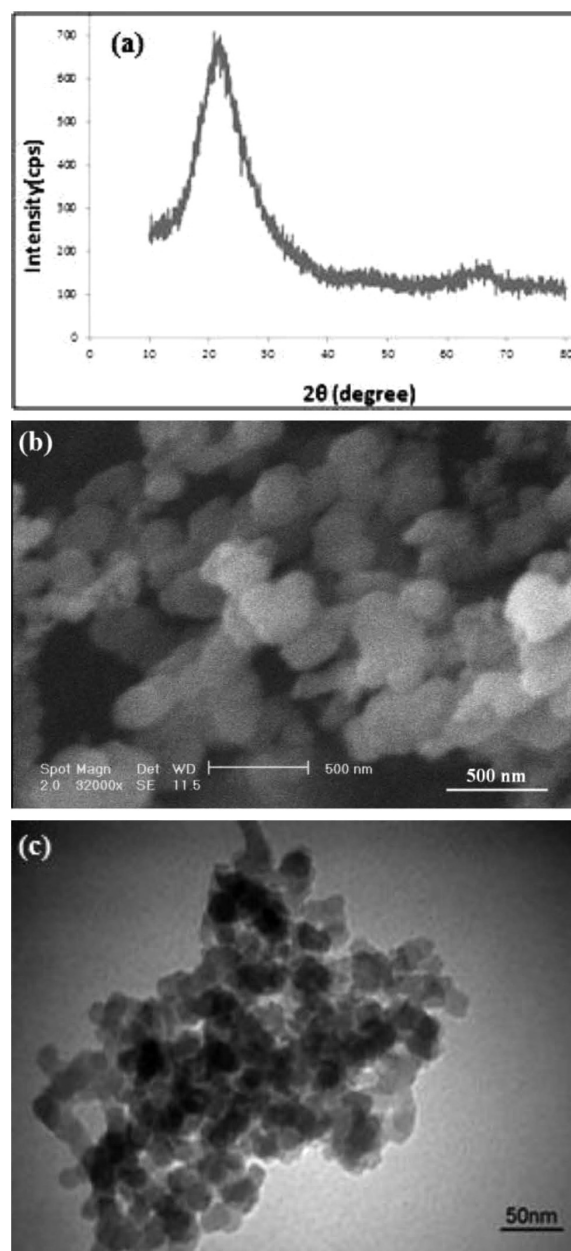


**Figure 1:** a) XRD pattern<sup>12</sup> b) SEM image, c) TEM image<sup>12</sup> from the powder resulted from pyrolysis and burning of HTV silicon polymer

diffraction pattern and the images of scanning electron and transmission electron microscopy.

To make molten AZ91C, first a burner furnace with natural gas fuel is used for melting the alloy and then a resistance furnace is used to maintain and control the temperature. The reason to select this method for melting the alloy was that the preparation of the molten alloy in the gas furnace is much quicker than in the resistance furnace. Therefore, by decreasing the molten alloy preparation time, one could prevent the oxidation of the molten alloy. As soon as the alloy is melted inside the gas furnace and for accurately controlling the temperature, the crucible of the molten alloy is transferred to the

electric furnace, which is warmed beforehand to reach the intended temperature and was close to the gas furnace. After reaching the desired temperature, the molten alloy is mixed. In **Figure 2**, the schematic picture of the stir casting system is shown.

To manufacture in-situ magnesium-matrix nano-composites AZ91C reinforced with oxide nano-particles, one kilograms of AZ91C magnesium bar and 20 g of nano-silica powder is prepared for each test. Then, holes with a diameter 13 millimeters are drilled into the magnesium bar. SiO<sub>2</sub> nano-powder mixed well with AZ91C alloy filings was put inside the holes and was pounded until the holes were filled with AZ91C filings. Then, the prepared set was put in a graphite crucible inside the furnace.

Unlike aluminum which has a continuous oxide layer and the oxide formation on the surface the molten aluminum prevents the contact between the molten material and air, magnesium oxide is porous and cannot make any protection of the molten material.<sup>3,5</sup> In the casting of magnesium alloy, if the metal and air contact is not cut during and after the melting, all the magnesium is oxidized and nothing but a white powder of magnesium oxide will remain. In stir casting in which the molten material is turbulent and has more contact with air, this issue is much more intense. In this study, to protect the AZ91C molten alloy, a mixture of carbon dioxide and argon with equal fractions is blown on the surface of the molten alloy and to mix it, a stirrer made out of simple carbon steel with three blades with 120° with respect to each other is used according to **Figure 3**. The thickness, width and length of the blades are (2, 15 and 20) mm, respectively. To increase the mixing power and create a more downward flow, blades with angles of 45 degrees were connected with respect to the mixing axis. To keep the molten alloy clean and increase the lifetime of the stirrer, the surface of the stirrer is coated with a nano-ceramic coating. While stirring, the stirrer is inserted into the molten alloy to half the height of the liquid.

After preparing the molten alloy, its temperature is raised to 750 °C and stirring is done for 15 min with a speed of 500 min<sup>-1</sup> so that the composite slurry is

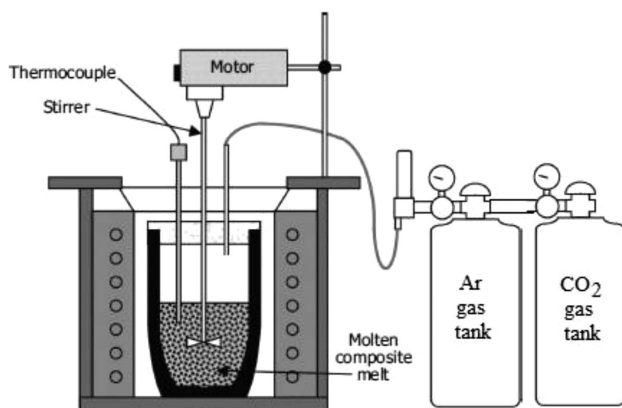


**Figure 2:** Schematic of the stir-casting system used in this research

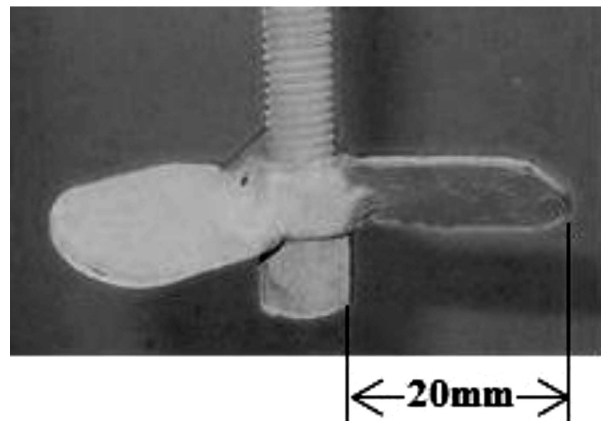


**Figure 3:** The picture of the stirrer used in this research

formed. Then, the temperature of the slurry was decreased to 720 °C and was poured into steel molds which were pre-warmed to 100 °C. The steel mold used which has four cylindrical holes as well as a cast sample is illustrated in **Figure 4**.

It should be noted that three composite samples consisting of 2 % of mass fractions of nano-silica powder were cast as described above and a non-composite sample made of AZ91C alloy was cast with similar conditions as the control sample. All the samples were lathed as the tensile test sample after cleaning based on ASTM-E8M standard<sup>13</sup> according to **Figure 5** to inves-



**Figure 4:** a) Steel mold used in this research, b) A cast sample in the mold



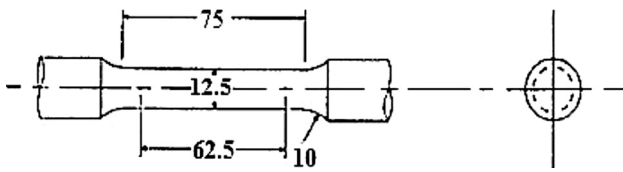


Figure 5: Schematic of the tensile test sample<sup>13</sup>

tigate the tensile properties. Preparing the sample for studying the micro-structures was performed according to the ASTM-E3-01 standard.<sup>14</sup> The surfaces of the samples were prepared in Nital Etch Solution 2 % and their microstructures were studied using a Mec 1042C light microscope.

### 3 RESULTS AND DISCUSSION

#### 3.1 Microstructural studies

Microstructural non-composite (control) and nano-composites samples are shown in **Figure 6** by optical microscopes. As observed in **Figures 6a** and **6b**, AZ91C alloy microstructures (control sample) consist of continuous intermetallic phase  $\beta$ -Mg<sub>17</sub>Al<sub>12</sub> which has surrounded the primary magnesium dendrites  $\alpha$ -Mg.  $\beta$ -Mg<sub>17</sub>Al<sub>12</sub> phase is mainly distributed along the boundaries of the primary phase  $\alpha$ -Mg grains and is in the shape of a long and continuous grid that leads to a reduction of the mechanical properties.

An important point when studying the nano-composite microstructures is to investigate the distribution and the bonds of the reinforcing particles in the matrix. Nevertheless, in **Figures 6c** and **6d** which display the nano-structures of the composite sample consisting of 2 % of mass fractions of nano-silica particles, there is no evidence of reinforcing particles in the matrix. Using nanometric reinforcing materials, when a proper distri-

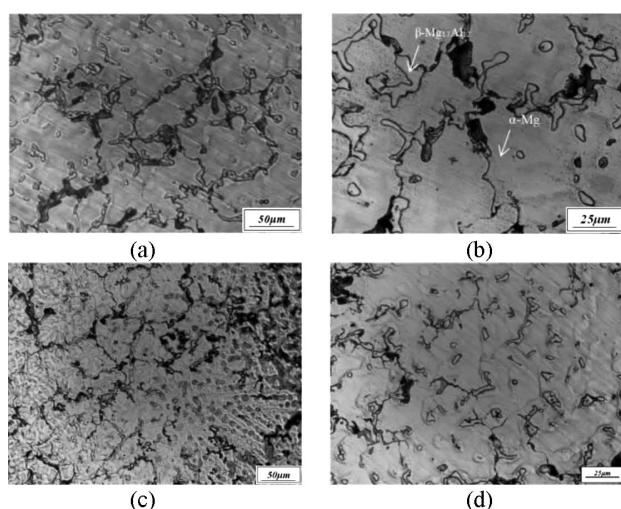


Figure 6: Light microscopic images in two different magnifications, a) and b) non-composite cast sample micro-structure, c) and d) composite cast micro-structure consisting of 2 % of reinforcing SiO<sub>2</sub> nano-particles

bution of the particles is achieved in the composite and large lumps of reinforcing material is not present in the structure, identifying and finding the reinforcing particles in the micro-structure is not possible with light microscopy and electronic microscopies are needed to study at higher magnifications. Also, indirect observations and studying the mechanical and physical properties could lead to understanding the presence and distribution of the reinforcements in the matrix.

**Figure 7** illustrates the Scanning Electron Microscopy (SEM) images for the composite sample consisting of 2 % of mass fractions SiO<sub>2</sub> reinforcing nano-particles. In this picture, particles with dimensions of tens to

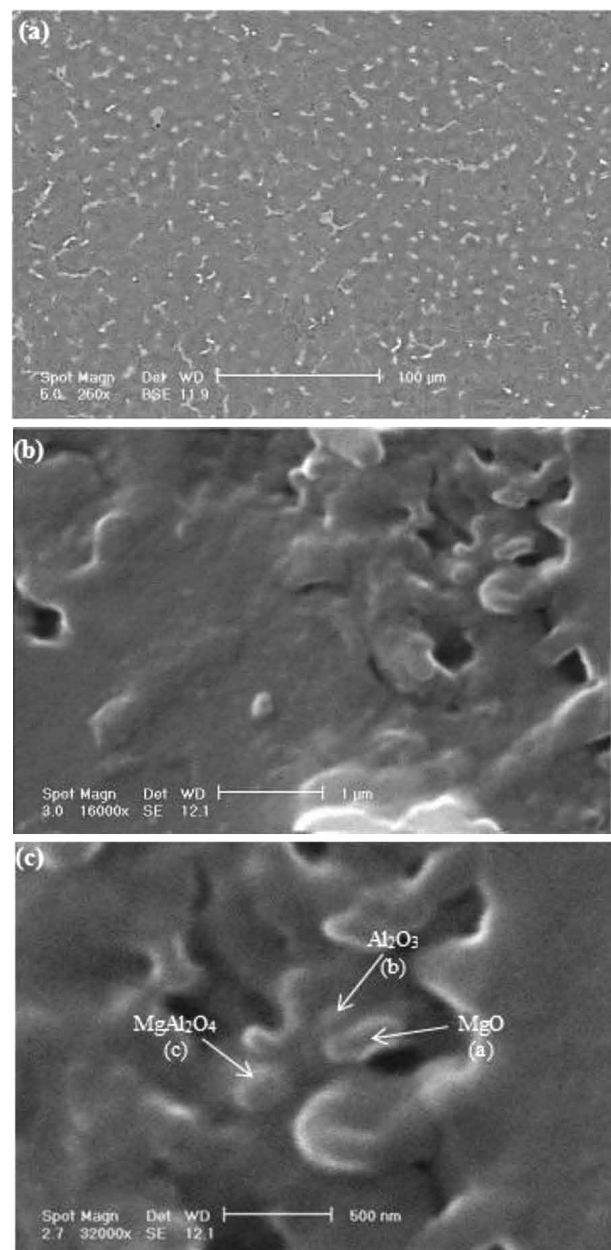


Figure 7: Scanning electron microscopy (SEM) images for the composite sample consisting of 2 % of mass fractions of SiO<sub>2</sub> reinforcing nano-particles

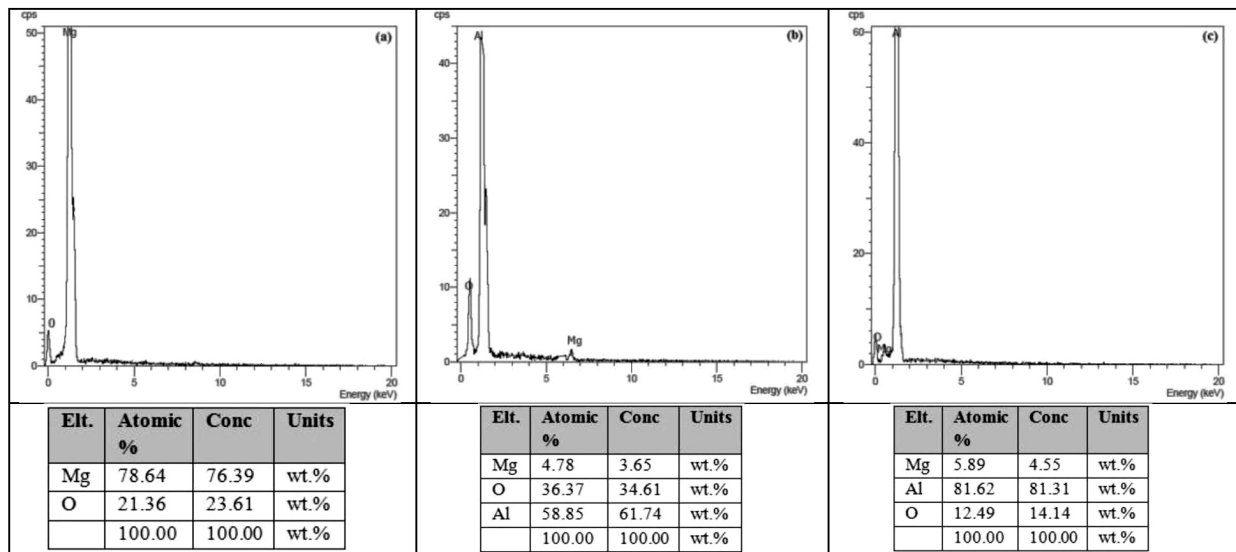


Figure 8: EDS elemental analysis from points a, b, and c

hundreds nanometers are observed. **Figure 8** shows the EDS analysis of the three specified phases of **Figure 7c**. According to this analysis, all the observed particles are oxidized and are made of  $\text{Al}_2\text{O}_3$ ,  $\text{MgO}$  and  $\text{MgAl}_2\text{O}_4$  and no sign of added nano-silica particles into the structure is observed. Therefore, it seems that the added nano-silica particles are reduced in the molten alloy and releasing oxygen has led to the in-situ creation of new oxide phases that are studied in what follows.

On the other hand, in **Figures 6c** and **6d**, it is observed that in AZ91C nano-composites, consisting of oxide nano-particles, the dendrites of the main phase  $\alpha$ -Mg have become finer and the shape of the initial phase has changed to equiaxed dendritic structure from a coarse dendritic form. It seems that the formed nano-particles in the molten alloy could have led to finer  $\alpha$ -Mg phase by creating the condition for better heterogeneous nucleation or effective prevention of the growth of grains, as well as modifying the continuous grids of phase  $\beta$ - $\text{Mg}_{17}\text{Al}_{12}$ .

### 3.2 Thermodynamic analysis of phase formations in the Mg-SiO<sub>2</sub> system

The chemical compound of the used alloy is presented in **Table 1** in which magnesium is the base metal and aluminum is the main alloying element. Moreover, during the procedure, nano-silica particles with high specific surface areas are added to the molten alloy at 750 °C, which are expected to create a good

condition for a reaction with the molten alloy. According Sreekumar et al.,<sup>17</sup> reactions 1 to 5 could occur between the main elements in the molten material and nano-silica particles. The released energy for each reaction at 750 °C (1023 K) is also shown next to each of them in **Table 2**.<sup>15–17</sup>

Since the released energy of all of these reactions is extremely negative at 750 °C, formation of  $\text{Al}_2\text{O}_3$ ,  $\text{MgAl}_2\text{O}_4$  and  $\text{MgO}$  phases, which are shown in **Figure 7c**, are thermodynamically feasible and spontaneous. The  $\text{MgAl}_2\text{O}_4$  phase shows a combination of unique properties such as low electrical conductivity, low thermal expansion coefficient, good thermal shock resistance, low dielectric constant, high electrical resistance, high melting point (2135 °C) and high mechanical strength.<sup>17,18</sup> Moreover, this compound has a good adhesion to metal matrices.<sup>19</sup> Various studies are carried out regarding the formation, interface type and crystallography of the  $\text{MgAl}_2\text{O}_4$  phase with reinforcements used in metal-matrix composites. The oxide reinforcements were used such as  $\text{Al}_2\text{O}_3$ , Saffil, Mullite, Kaowool,  $\text{Al}_4\text{B}_3\text{O}_{18}$ ,  $\text{MgO}$ , ASZ (Composition  $\text{Al}_2\text{O}_3$ ,  $\text{SiO}_2$  and  $\text{ZrO}_2$  in 3 : 5 : 2 ratio and are amorphous in their as-fabricated state) and glass fibers or non-oxide reinforcements such as graphite,  $\text{B}_4\text{C}$ ,  $\text{AlN}$  and  $\text{SiC}$ . Studying the reactions with oxide reinforcements has shown that  $\text{MgAl}_2\text{O}_4$  is formed due to the reaction of the oxide reinforcements with aluminum and magnesium in the matrix alloy. Also, the oxidation of the volatile surface of non-oxide reinforcements leads

Table 2: Reactions could occur between the main elements in the molten material and nano-silica particles

(1)	$\Delta G_{1023\text{ K}}^0 = -348.19 \text{ kJ/mol}$	$4\text{Mg(l)} + \text{SiO}_2(\text{s}) \rightarrow \text{Mg}_2\text{Si(s)} + 2\text{MgO(s)}$
(2)	$\Delta G_{1023\text{ K}}^0 = -268.22 \text{ kJ/mol}$	$\text{SiO}_2(\text{s}) + 2\text{Mg(l)} \rightarrow 2\text{MgO(s)} + \text{Si(l)}$
(3)	$\Delta G_{1023\text{ K}}^0 = -449.63 \text{ kJ/mol}$	$2\text{SiO}_2(\text{s}) + \text{Mg(l)} + 2\text{Al(l)} \rightarrow \text{MgAl}_2\text{O}_4(\text{s}) + 2\text{Si(l)}$
(4)	$\Delta G_{1023\text{ K}}^0 = -556.44 \text{ kJ/mol}$	$3\text{SiO}_2(\text{s}) + 4\text{Al(l)} \rightarrow 2\text{Al}_2\text{O}_3(\text{s}) + 3\text{Si(l)}$
(5)	$\Delta G_{1023\text{ K}}^0 = -631.08 \text{ kJ/mol}$	$3\text{SiO}_2(\text{s}) + 2\text{MgO(s)} + 4\text{Al(l)} \rightarrow 2\text{MgAl}_2\text{O}_4(\text{s}) + 3\text{Si(l)}$

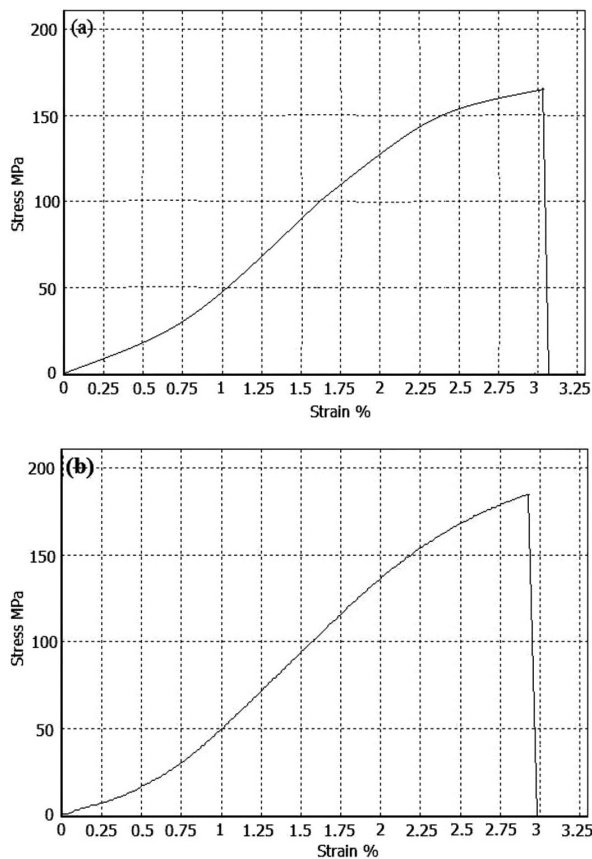


**Figure 9:** An example of stress-strain curves resulted from tensile test for: a) non-composite samples, b) composite samples

to the formation of a reactive oxide layer, which helps the formation of  $MgAl_2O_4$ . The formation of  $SiO_2$  on  $SiC$ ,  $Al_2O_3$  on  $AlN$  and  $B_2O_3$  on  $B_4C$  are the examples of this mechanism.<sup>17</sup> In some cases it is reported that the absorption of the oxygen on the surface of the reinforcements acts as a source for the formation of  $MgAl_2O_4$ .<sup>19</sup>  $Al_2O_3$  has rigidity and high strength as well as corrosion resistance and sufficient thermal stability.<sup>20</sup> Magnesium composites reinforced with  $Al_2O_3$  nano-particles show a considerable increase in the microhardness and a slight increase in the elasticity modulus and yield strength.<sup>21</sup> The hardness and tensile strength increase in the AZ91 alloy reinforced with  $MgO$ .<sup>22</sup>

### 3.3 Investigating the mechanical properties

**Figure 9** shows an example of stress-strain curves resulting from the tensile test for composite and non-

composite samples. The average values of the mechanical properties including hardness, yield strength, ultimate tensile strength and elongation percentage of the non-composite sample and nano-composite samples are shown in **Table 3**.

As observed in **Figure 9** and **Table 3**, hardness, yield strength and ultimate tensile strength of the cast nano-composite samples increased compared to the cast non-composite sample (control sample) and their elongation percentage has slightly decreased.

Different mechanisms are presented for improving the mechanical properties of the metal-matrix composites. Examining the shapes and sizes of the grains and the properties of the composite samples, one could understand the effectiveness of the operation. One of the evidences of the improvement of the properties in the composite samples is that the microstructures of the cast nano-composite samples have finer and more uniform grains compared to the non-composite samples (Hall-Petch effect). Also, the secondary phase  $\beta-Mg_{17}Al_{12}$  is considerably crushed in the grain boundaries of the primary phase, has lost its continuity and is distributed more uniformly in the structure. It seems that the reason for this is the uniform distribution of the reinforcing particles in the structure and their effect on the nucleation of the primary phase and preventing the growth of the grains. Another impact is the formation of oxide nano-particles in the matrix such that they are almost homogeneously distributed in the matrix. As observed in **Figure 6**, the distribution and how the reinforcing nano-particles are put together are not clear in this picture, which shows the relatively proper distribution of the reinforcing particles and the absence of large lumps in the matrix.

A. Sanati Zadeh et al.<sup>23</sup> found the Hall-Petch strengthening effect to be very important for the strength of nano-composites such that it causes up to 50 % of the total strengthening.

As the elasticity modulus of the matrix and reinforcement are completely different, when one-dimensional loading is applied on a composite material, a combined stress distribution is formed. Highly accurate analyses show that shear stresses occur in the boundary of the matrix with the particles, which leads to an increased strength.<sup>24</sup>

As shown in **Figure 8** and **Table 3**, while the strengths of the composite samples are increased, their elongation percentages are somewhat decreased. This is generally observed in composites. In fact, the same

**Table 3:** Mechanical properties of non-composite and nano-composite samples

% Nano silica	Hardness (BHN)	U.T.S (MPa)	Y.S (MPa)	% El	
0	5±65	3±165	2±82	0.3±3.5	Non-composite sample (control sample)
2	3±77	2±175	3±97	0.2±3	Nano-composite sample (average of three tests)
-	+18.5	+6.1	+18.3	-14.3	Percent change



mechanisms which lead to an increased strength, decrease the deformation of the matrix as well. Moreover, the weak bond between the reinforcing particles and magnesium matrix and defects such as gaseous pores could also be factoring, which leads to a more intense decrease of the flexibility of the composites.

#### 4 CONCLUSION

An AZ91C nano-composite consisting of  $\text{Al}_2\text{O}_3$ ,  $\text{MgAl}_2\text{O}_4$  and  $\text{MgO}$  oxide nano-particles is successfully produced using the stir-casting method. The existence of  $\text{Al}_2\text{O}_3$ ,  $\text{MgAl}_2\text{O}_4$  and  $\text{MgO}$  oxide particles in an AZ91C alloy has a proper reinforcing role and the manufactured nano-composites have finer and more uniform grains compared to the non-composite control sample. Also, the secondary phase  $\beta\text{-Mg}_{17}\text{Al}_{12}$  is fairly crushed and is distributed in a non-continuous form in the structure. These changes lead to the improvement of the mechanical properties compared to the non-composite control sample so that the hardness, yield strength and tensile strength are increased from 65 BHN, 82 MPa and 165 MPa in the non-composite sample to 77 BHN, 97 MPa and 175 MPa in the composite sample.

#### Acknowledgements

The authors are grateful for support of this research by Isfahan University of Technology (IUT).

#### 5 REFERENCES

- E. F. Horst, L. M. Barry, *Magnesium Technology* (Metallurgy, Design Data, Applications), Springer, Germany, (2006)
- M. Gupta, N. M. L. Sharon, *Magnesium, Magnesium Alloys, and Magnesium Composites*, John Wiley & Sons, Inc., New Jersey, (2011)
- A. W. Brace, F. A. Allen, *Magnesium Casting Technology*, London, Chapman & Hall; New York, Reinhold Pub. Corp., (1957)
- ASM Handbook Committee, *Metals Handbook*, Vol. 15, casting, ASM International, Ten Edition, (2008)
- H. E. Friedrich, B. L. Mordike, *Magnesium Technology* (Metallurgy, Design Data, Applications), 1<sup>st</sup> Ed., Springer, Germany, (2006)
- S. F. Hassan, M. Gupta, Effect of submicron size  $\text{Al}_2\text{O}_3$  particulates on microstructural and tensile properties of elemental Mg. *Journal of Alloys and Compounds*, 457 (2008), 244–250, doi:10.1016/j.jallcom.2007.03.058
- D. Vollath, *Nanomaterials: An Introduction to Synthesis, Properties and Applications*, 2nd Edition, (2013)
- H. Choi, Y. Sun, B. P. Slater, H. Konishi, X. Li, AZ91D-TiB<sub>2</sub> Nanocomposites Fabricated by Solidification Nanoprocessing, *Advanced Engineering Materials*, 14 (2012) 5, 291–295, doi:10.1002/adem.201100313
- M. Habibnejad-Korayem, R. Mahmudi, W. J. Poole, Enhanced properties of Mg-based nanocomposites reinforced with  $\text{Al}_2\text{O}_3$  nano particles, *Materials Science and Engineering A*, 519 (2009), 198–203, doi:10.1016/j.msea.2009.05.001
- K. Kainer, *Metal matrix composite*, Wiley book, (2006)
- International ASTM B 80-05, Standard specification for magnesium –alloy sand casting, (2005)
- M. Senemar, A. Maleki, B. Niroumand, A. Allafchian, A Novel And Facile Method For Silica Nanoparticles Synthesis From High Temperature Vulcanization (HTV) Silicone, *Association of Metallurgical Engineers of Serbia (AMES)*, 22 (2016) 1, 1–8, <https://metall-mater-eng.com/index.php/home/article/view/134/120>
- International ASTM B E8/E8M – 09, Standard Test Methods for Tension Testing of Metallic Materials1, (2010)
- International ASTM E03-1, Standard Practice for Preparation of Metallographic Specimens, (2007)
- D. Huang, Y. Wang, Y. Wang, H. Cui, X. Guo, In situ  $\text{Mg}_2\text{Si}$  reinforced Mg alloy synthesized in Mg-SiO<sub>2</sub> system, *Advanced Materials Research*, 146–147 (2011), 1775–1779, doi:10.4028/www.scientific.net/AMR.146-147.1775
- Y. J. Liang, Y. C. Chen, *Thermodynamic Data Handbook on Inorganic Substances*, Dongbei University Press, China, in Chinese, (1993)
- V. M. Sreekumar, R. M. Pillai, B. C. Pai, M. Chakraborty, Evolution of  $\text{MgAl}_2\text{O}_4$  crystals in Al-Mg-SiO<sub>2</sub> composites, *Applied Physics A Materials Science & Processing*, A 90 (2008), 745–752, doi:10.1007/s00339-007-4357-2
- C. Pacurariu, I. Lazau, Z. Ecsedi, R. Lazau, P. Barvinschi, G. Marginean, New synthesis methods of  $\text{MgAl}_2\text{O}_4$  spinel, *Journal of the European Ceramic Society*, 27 (2007), 707–710, doi:10.1016/j.jeurceramsoc.2006.04.050
- G. Ramani, R. M. Pillai, B. C. Pai, T. R. Ramamohan, Factors affecting the stability of non-wetting dispersed suspensions in metallic melts, *Composites*, 22 (1991) 2, 143–150, doi:10.1016/0010-4361(91)90673-5
- A. Kazunori, Y. Hiroyuki, Effects of Particle-Dispersion on the Strength of an Alumina Fiber-Reinforced Aluminum Alloy Matrix Composite, *Materials Transactions*, 44 (2003) 6, 1172–1180, <https://www.jim.or.jp/journal/e/pdf3/44/06/1172.pdf>
- T. S. Srivatsan, C. Godbole, T. Quick, M. Paramsothy, M. Gupta, Mechanical Behavior of a Magnesium Alloy Nanocomposite Under Conditions of Static Tension and Dynamic Fatigue, *Journal of Materials Engineering and Performance*, 22 (2013), 439–453, doi:10.1007/s11665-012-0276-2
- Z. Song-li, Z. Yu-tao, C. Gang, In situ ( $\text{Mg}_2\text{Si}+\text{MgO}$ )/Mg composites fabricated from AZ91- $\text{Al}_2(\text{SiO}_3)_3$  with assistance of high-energy ultrasonic field, *Transactions of Nonferrous metals Society of china*, 20 (2010), 2096–2099, doi:10.1016/S1003-6326(09)60424-6
- A. Sanaty-Zadeh, P. K. Rohatgi, Comparison between Current Models for the Strength of Particulate Reinforced Metal Matrix Nanocomposites with Emphasis on Consideration of Hall–Petch Effect, *Materials Science and Engineering, A* 531(2012), 112–118, doi:10.1016/j.msea.2011.10.043
- G. E. Dieter, *Mechanical Metallurgy*, MacGraw-Hill Book Company Limited, UK, (1988)